



Mast Cell Cytonemes as a Defense Mechanism against *Coxiella burnetii*

Soraya Mezouar,^a Joana Vitte,^{a,b} Laurent Gorvel,^c Amira Ben Amara,^c Benoit Desnues,^a Jean-Louis Mege^{a,b}

^aAix-Marseille Université, IRD, APHM, MEPHI, IHU-Méditerranée Infection, Marseille, France

^bAPHM, IHU-Méditerranée Infection, UF Immunologie, Marseille, France

^cCRCM, CNRS UMR7258, INSERM U1068, Institut Paoli-Calmettes, Aix-Marseille Université, UM105, Marseille, France

ABSTRACT Mast cells (MCs) are critical mediators of inflammation; however, their microbicidal activity against invading pathogens remains largely unknown. Here, we describe a nonpreviously reported antibacterial mechanism used by MCs against *Coxiella burnetii*, the agent of Q fever. We show that *C. burnetii* interaction with MCs does not result in bacterial uptake but rather induces the formation of extracellular actin filaments named cytonemes. MC cytonemes express cathelicidin and neutrophil elastase and mediate the capture and destruction of entrapped bacteria. We provide evidence that MC cytoneme formation and microbicidal activity are dependent on the cooperation of the scavenger receptor CD36 and Toll-like receptor 4. Taken together, our results suggest that MCs use an extracellular sophisticated mechanism of defense to eliminate intracellular pathogens, such as *C. burnetii*, before their entry into host cells.

IMPORTANCE Mast cells (MCs) are found in tissues that are in close contact with external environment, such as skin, lungs, or intestinal mucosa but also in the placenta during pregnancy. If their role in mediating allergic conditions is established, several studies now highlight their importance during infection with extracellular pathogens. This study showed a new and effective antimicrobial mechanism of MCs against *Coxiella burnetii*, an intracellular bacterium whose infection during pregnancy is associated with abortion, preterm labor, and stillbirth. The data reveal that in response to *C. burnetii*, MCs release extracellular actin filaments that contain antimicrobial agents and are capable to trap and kill bacteria. We show that this mechanism is dependent on the cooperation of two membrane receptors, CD36 and Toll-like receptor 4, and may occur in the placenta during pregnancy by using *ex vivo* placental MCs. Overall, this study reports an unexpected role for MCs during infection with intracellular bacteria and suggests that MC response to *C. burnetii* infection is a protective defense mechanism during pregnancy.

KEYWORDS CD36, *Coxiella burnetii*, mast cells, TLR4, cytonemes

Mast cells (MCs) are hematopoietic cells residing in tissues that occupy a strategic position at host-environment interfaces, such as skin and mucosae. They are characterized by a high content of electron-dense secretory granules containing high-performance mediators, such as histamine, amines, serotonin, and proteases, such as trypsin and chymase, and express CD117 (c-kit) and IgE (FcεR1) receptors (1). They are well-known as immune effectors of anaphylaxis, but their role in defending against pathogens is emerging. MCs contribute to antibacterial immunity via multiple mechanisms. They are equipped with microbial sensors, such as Toll-like receptors (TLRs), including TLR2 and TLR4, and are involved in the recognition of Gram-positive and -negative bacteria (2–4). In response to lipopolysaccharide (LPS) or bacterial pathogens, MCs release inflammatory cytokines that mediate the recruitment of immune cells and

Citation Mezouar S, Vitte J, Gorvel L, Ben Amara A, Desnues B, Mege J-L. 2019. Mast cell cytonemes as a defense mechanism against *Coxiella burnetii*. mBio 10:e02669-18. <https://doi.org/10.1128/mBio.02669-18>.

Editor Jon P. Boyle, University of Pittsburgh

Copyright © 2019 Mezouar et al. This is an open-access article distributed under the terms of the [Creative Commons Attribution 4.0 International license](https://creativecommons.org/licenses/by/4.0/).

Address correspondence to Jean-Louis Mege, jean-louis.mege@univ-amu.fr.

Received 30 November 2018

Accepted 1 March 2019

Published 16 April 2019

secrete antimicrobial agents, including cathelicidin (LL-37) and neutrophil elastase (5). MCs are able to ingest and kill extracellular bacteria, such as *Staphylococcus aureus*, through an endosome-lysosome pathway (6) or to use an extracellular antimicrobial mechanism consisting of the release of extracellular traps (ETs) (7). Similarly to those formed by neutrophils, these ETs are composed of antimicrobial peptide-lined DNA projections, allowing the rapid immobilization and killing of microorganisms (7).

Coxiella burnetii is an intracellular bacterium responsible for Q fever, an acute infectious disease that may become persistent in specific clinical contexts (8). In myeloid cells, such as monocytes/macrophages and dendritic cells, *C. burnetii* survives and replicates, but it has nevertheless been shown to infect other cell types, including trophoblasts and adipocytes (9–12). *C. burnetii* is recognized by myeloid cells through $\alpha\text{v}\beta\text{3}$ integrin and TLR2/TLR4-dependent mechanism, leading to cytokine production and cytoskeleton reorganization (13, 14). *C. burnetii* is also able to subvert immune responses by interfering with uptake mechanisms and phagosome biogenesis (15), stimulating the production of interleukin-10 (IL-10), and promoting the expansion of regulatory T cells (13).

In the present study, we report that MCs were microbicidal for the intracellular pathogen *C. burnetii* through a nonpreviously reported mechanism. Indeed, MCs have released cytonemes consisting of long extensions of F-actin enriched with cathelicidin and neutrophil elastase. These structures trapped and killed *C. burnetii* organisms. Cytoneme-mediated killing of *C. burnetii* was under the control of the cross talk between TLR4 and CD36. These results suggest that MCs have shaped an extracellular sophisticated mechanism of defense to eliminate intracellular pathogens before their entry in immune cells.

RESULTS

MCs kill *C. burnetii* through an extracellular mechanism. HMC-1.2 cells were incubated with *C. burnetii* (50 bacteria per cell) for different periods of time, and the number of bacterial DNA copies was determined by qPCR. After 3 h of infection, more than 10 (7) *C. burnetii* DNA copies were detected. This number markedly decreased by 90% after 24 and 48 h (Fig. 1A). We questioned whether the decrease in the number of bacterial DNA copies reflected the uptake and elimination of bacteria by MCs. We assessed the uptake of *C. burnetii* by confocal microscopy, using *S. aureus* as the control. *S. aureus* organisms were found within MCs at 3 h postinfection (p.i.), and the bacterial burden increased at 24 h p.i. (Fig. 1B). In contrast, no *C. burnetii* organisms were found within MCs at 3 and 24 h p.i, as opposed to monocytes which are permissive cells for *C. burnetii* (see Fig. S1 in the supplemental material) as we previously described (16). It is noteworthy that some *C. burnetii* organisms were observed at the surfaces of MCs with intense F-actin rearrangements (Fig. 1B). The decreased number of *C. burnetii* DNA copies and the defective uptake of bacteria suggested that an extracellular antimicrobial mechanism was employed by MCs to eliminate *C. burnetii*. Since ETs are used by neutrophils and MCs to eliminate different types of bacteria (7), we quantified the release of ETs in response to *C. burnetii* and *S. aureus* and used PMA as a positive control. In neutrophils, *C. burnetii* and *S. aureus* induced a release of ETs similar to that induced by PMA (Fig. 1C). In MCs, *S. aureus* triggered intense formation of ETs as in neutrophils, whereas *C. burnetii* induced the release of few ETs (Fig. 1D). Therefore, we wondered whether these rare traps were sufficient to eliminate *C. burnetii* organisms. For that purpose, we treated *C. burnetii*-incubated MCs with DNase, which is known to disrupt ETs (17). This treatment did not increase the number of intracellular *C. burnetii* DNA copies, suggesting that another extracellular mechanism is involved in the trapping and elimination of *C. burnetii* by MCs (Fig. 1E). Taken together, these results suggested that MCs use an ET-independent extracellular mechanism to kill *C. burnetii*.

***C. burnetii* induces the formation of cytonemes by MCs.** As *C. burnetii* markedly remodeled MC cytoskeleton, we analyzed the F-actin rearrangements induced by bacteria. We observed the release of extracellular thread-like membrane actin filaments (Fig. 2A). These structures were predominantly linear and distinct from pseudopods.

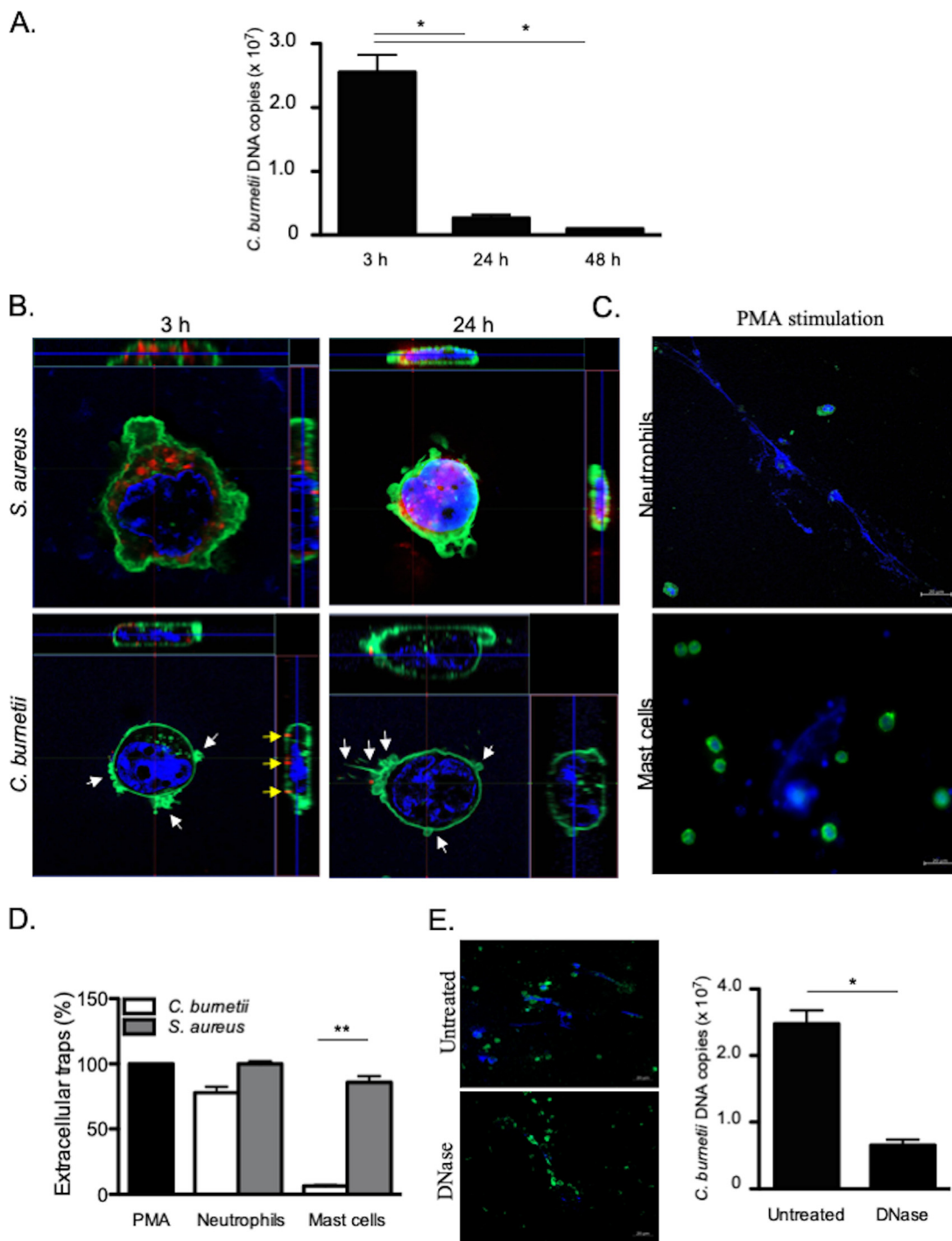


FIG 1 Extracellular killing of *C. burnetii*. HMC-1.2 cells (1×10^6) were incubated with *C. burnetii* (50 bacteria per cell) for different periods of time. (A) After the cells were washed, the number of *C. burnetii* DNA copies was determined by qPCR. (B) Confocal sections of MCs incubated with *S. aureus* (top panel) or *C. burnetii* (bottom panel). Bacteria (red), F-actin (green), nucleus (blue), and cytoskeletal reorganization (white arrows) are indicated. Bacteria located on the MC membrane are represented by yellow arrows. (C and D) The extracellular traps released by neutrophils or MCs incubated with PMA, *C. burnetii*, or *S. aureus* for 3 h were observed (DNA in blue and F-actin in green) (C) and quantified by evaluating the release of fluorescent DNA (D). The results, expressed as relative to PMA-stimulated cells, are the means plus standard deviations (SD) (error bars) for triplicate samples from at least three independent experiments. **, $P \leq 0.01$. (E) The number of *C. burnetii* DNA copies was determined by qPCR in MCs incubated with bacteria for 3 h and then treated with 50 U/ml DNase for 10 min to eliminate ETs. The results are expressed as the means plus SD for triplicate samples from at least three independent experiments. *, $P \leq 0.05$.

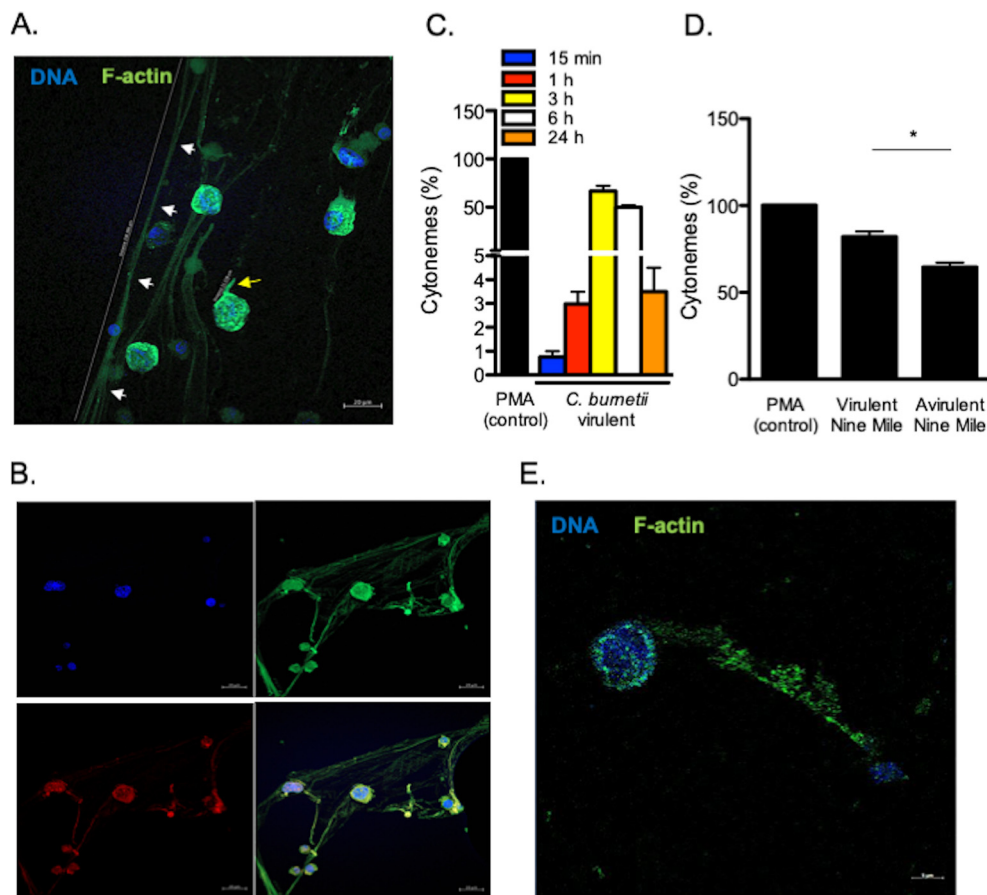


FIG 2 *C. burnetii*-induced formation of cytonemes. (A) Cytonemes (white arrows, distance 208.4 μm) and pseudopods (yellow arrow, distance 11.1 μm) stained with indicated markers were observed by confocal microscopy in MCs stimulated for 3 h. (B) Tubulin (red), F-actin (green), and DNA (blue) staining were evaluated on cytonemes. (C) The formation of cytonemes by MCs was quantified after stimulation with *C. burnetii* and expressed as a percentage relative to PMA as the positive control. (D) The formation of cytonemes was quantified after a 3-h incubation of MCs with virulent (Nine Mile) and avirulent (Nine Mile variant) bacteria. The results are expressed as a percentage relative to PMA stimulation. (E) The release of cytonemes by pMCs stimulated by *C. burnetii* for 3 h was observed by confocal microscopy, stained with the indicated markers. The results are expressed as the means plus SD for triplicate samples from four independent experiments. *, $P \leq 0.05$.

They measured up to 200 μm in length and were composed of F-actin and tubulin (Fig. 2B), suggesting that they were similar to the cytonemes produced by MCs as previously described (18). The cytonemes appeared 15 min after *C. burnetii* stimulation; the number of cytonemes reached a maximum between 3 and 6 h ($\geq 50\%$) and decreased thereafter (Fig. 2C). Several strains of *C. burnetii* have been described: they include the Nine Mile strain (the reference strain) and Guyana strain (the most virulent). We previously observed intense cell projections from monocytes stimulated by virulent *C. burnetii* compared to the avirulent variant (19). We wondered whether cytoneme formation was related to the virulence of *C. burnetii*. Avirulent variants of the Nine Mile strain poorly induced the formation of cytonemes compared to the virulent Nine Mile strain (Fig. 2D). Interestingly, the Guyana strain induced a significant increase of cytonemes formation compared to the PMA control (Fig. S2).

As the formation of cytonemes was observed with a MC line, we wondered whether primary MCs responded similarly to *C. burnetii*. Therefore, we purified MCs from placenta, a tissue for which *C. burnetii* has a strong tropism (20). The placental MCs (pMCs) were identified by flow cytometry using $\text{Fc}\epsilon\text{R1}^+/\text{CD117}^+$ (Fig. S3A) and tryptase staining (Fig. S3B). These pMCs were characterized by an ovoid nucleus, an irregular membrane, a metachromatic staining of granules, and the presence of several tryptase-

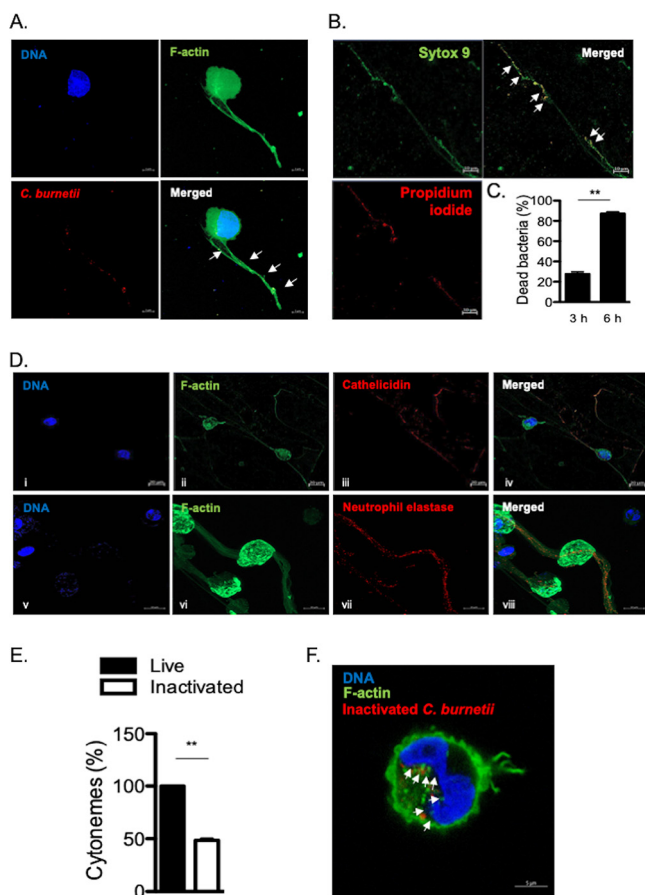


FIG 3 Cytonemes trap and kill *C. burnetii*. HMC-1.2 cells were incubated with *C. burnetii* (Nine Mile strain) for 3 h. (A) Bacteria (white arrows), colocalizing with cytonemes, appeared in yellow. (B) Bacteria entrapped in cytonemes were indicated with white arrows. Their viability was studied by immunofluorescence microscopy: Live bacteria were stained with Sytox 9 and appeared in green, whereas dead bacteria were stained with propidium staining and appeared in red. (C) The viability of bacteria entrapped in cytonemes was quantified at 3 and 6 h p.i. (D) Cathelicidin and neutrophil elastase were stained with specific Abs and were observed in red on MC cytonemes infected with *C. burnetii* with F-actin labeled in green and DNA in blue. (E) The percentage of cytonemes induced by heat-inactivated bacteria is expressed relative to the number of cytonemes induced by living bacteria. (F) The heat-inactivated bacteria were labeled in red within MCs (white arrows). F-actin and DNA are shown in green and blue, respectively. Data are the means plus SD for triplicate samples from three independent experiments. **, $P \leq 0.01$.

positive cytoplasmic granules using MGG and toluidine blue (Fig. S3C), electron microscopy (Fig. S3D) and immunofluorescence (Fig. S3E). As observed for the MC cell line, *C. burnetii* also induced the formation of cytonemes in primary MCs (Fig. 2E). Altogether, these findings show that *C. burnetii* induces the formation of cytonemes by MCs and suggest that this phenotype depends, at least in part, on the virulence of the bacteria.

MC cytonemes capture and kill bacteria. In order to understand the role of cytonemes in the MC response to *C. burnetii*, we incubated MCs with bacteria. We found that organisms were entrapped in cytonemes (Fig. 3A). After 3 h of contact between MCs and bacteria, approximately 20% of *C. burnetii* organisms were already dead and this number reached 80% after 6 h with the use of propidium iodide staining (Fig. 3B and C), suggesting that cytonemes were involved in *C. burnetii* killing. As MCs are known to secrete several antimicrobial products, we investigated their presence in cytonemes. MCs were incubated with *C. burnetii* for 3 h, and the distribution of antimicrobial agents, such as cathelicidin or neutrophil elastase, and extracellular F-actin, was studied by confocal microscopy. We found that both cathelicidin and

neutrophil elastase colocalized with cytonemes (Fig. 3D), demonstrating that cytonemes were armed to kill entrapped bacteria.

Second, we wondered whether cytonemes may protect MCs by avoiding the internalization of virulent organisms. When MCs were incubated with heat-inactivated *C. burnetii* instead of living bacteria, cytoneme formation was significantly ($P = 0.0042$) reduced (Fig. 3E). Interestingly, we found that heat-inactivated bacteria were found inside MCs (Fig. 3F), suggesting that cytoneme formation was associated with restricted uptake of bacterial pathogens. Taken together, these results highlight the role of cytonemes in killing virulent *C. burnetii* and represent another way other than phagocytosis in MCs.

Specific transcriptomic signature of *C. burnetii*-stimulated MCs. To understand the molecular pathways involved in the formation of MC cytonemes, we studied the transcriptional signature of MCs stimulated with *C. burnetii* by whole-genome microarray. Hierarchical clustering revealed a specific pattern for MCs stimulated with virulent bacteria that induced the formation of cytonemes, whereas MCs stimulated with an avirulent variant clustered with unstimulated MCs (Fig. 4A). Principal-component analysis confirmed that the signatures of MCs, stimulated with virulent and avirulent bacteria, were clearly distinct (Fig. 4B). We found that 56 genes were differentially expressed in response to *C. burnetii*, and most of these genes were upregulated in response to virulent organisms, whereas downregulated genes were prominent in response to the avirulent variant (Fig. 4C). Genes involved in several biological processes were enriched using the Gene Ontology (GO) Consortium approach. They included genes involved in cytoskeleton organization, cytokine-mediated signaling, immune response, metabolic process, ion transport, transcription, apoptosis, cell adhesion, cell-cell signaling, and cell projection (Fig. 4D). Therefore, to validate our findings, we selected 10 genes (*TMEM231*, *OCRL*, *CYLD*, *IL36G*, *TRIM62*, *LNX1*, *DST*, *PRRG1*, *CENPJ*, and *RALGPS2*) for which we assessed the modulation by qRT-PCR (see Table S2 in the supplemental material).

Interaction of CD36 with TLR4 in *C. burnetii* cell infection. Among the modulated genes, we found that the gene encoding CD36 was found in three GO terms, including cell projection, immune response, and cytoskeleton organization, and its expression was upregulated in response to virulent bacteria compared to the avirulent variant (Fig. 4E). The analysis of CD36 expression by qRT-PCR and flow cytometry confirmed microarray data and showed that CD36 expression was increased only in MCs stimulated with virulent bacteria (Fig. 5A and B). The confocal microscopy analysis revealed that CD36 was overexpressed as membrane clusters in MCs stimulated with *C. burnetii* (Fig. 5C). In addition, CD36 colocalized with *C. burnetii* at the surfaces of MCs (Fig. 5D). As CD36 is known to cooperate with TLRs to clear microbial infection (21) and TLR4 has been involved in actin remodeling in myeloid cells during *C. burnetii* infection (22), we investigated the expression of TLR2 and TLR4 in stimulated MCs. The expression of the *TLR4* gene, but not that of the *TLR2* gene, was dramatically upregulated in response to *C. burnetii*, as measured by qRT-PCR (Fig. 5E) and flow cytometry (Fig. 5F). In a second step, we wondered whether CD36 and TLR4 were associated in MCs stimulated by *C. burnetii*. Image overlay obtained by confocal microscopy showed that membrane CD36 and TLR4 colocalized at the surfaces of MCs incubated with *C. burnetii* (Fig. 5G). The direct interaction between CD36 and TLR4 was then assessed by immunoprecipitation experiment. We found that CD36 immunoprecipitated with TLR4 with a maximal intensity 1 h after incubation of MCs with *C. burnetii* (Fig. 5H). The cross talk between CD36 and TLR4 was further confirmed by inhibition experiments. First, inhibition of CD36 with blocking Abs (Fig. 5J) or transfection of MCs with a siRNA directed against *CD36* (Fig. S4), significantly reduced the expression of *TLR4* in stimulated MCs (Fig. 5I). In addition, polymyxin B, an inhibitor of LPS binding, reduced *TLR4* and *CD36* expression of *C. burnetii*-stimulated cells. Finally, in TLR4-deficient BMdMCs stimulated by *C. burnetii*, the expression of *CD36* was severely impaired compared to wild-type

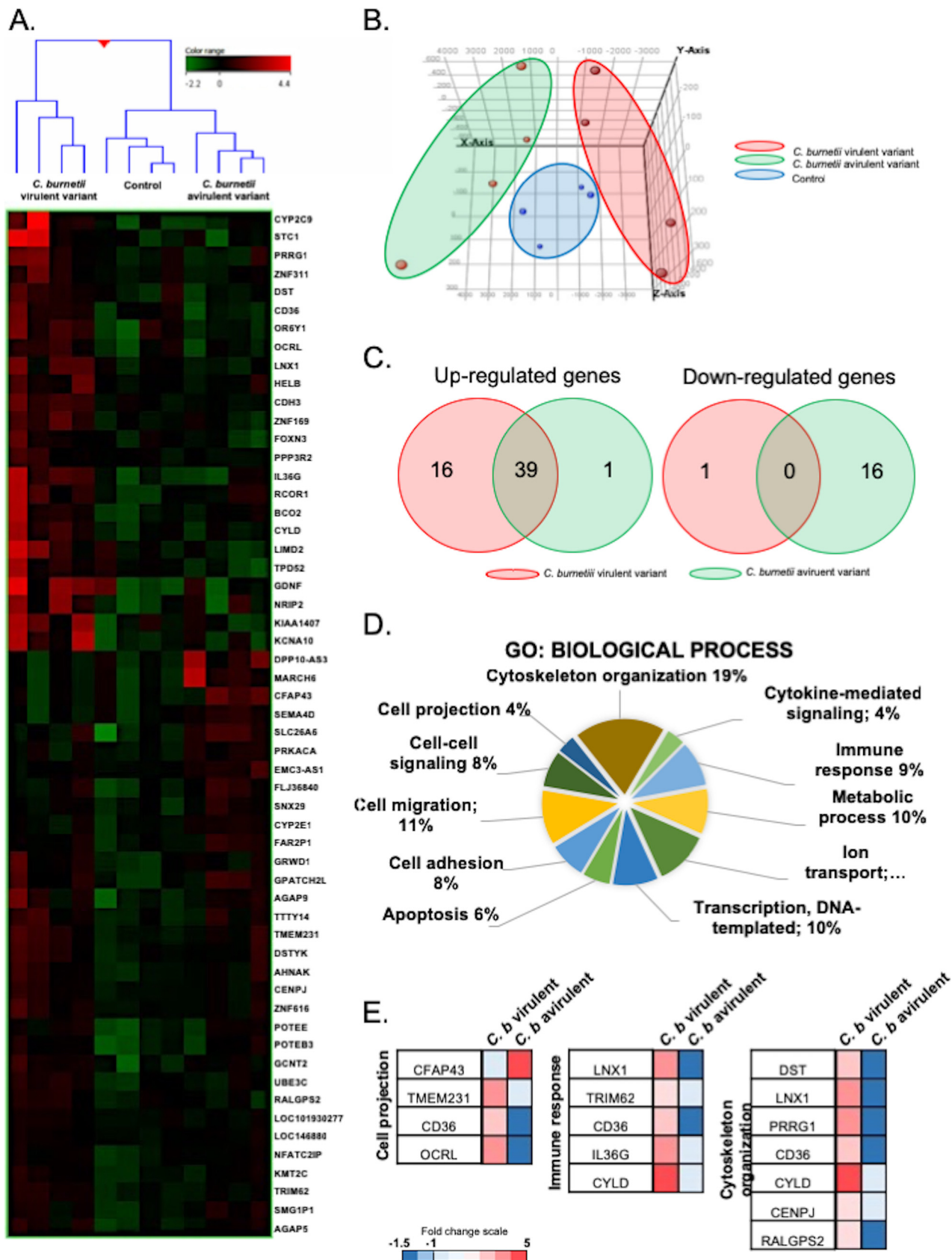


FIG 4 Transcriptional signature of MCs in response to *C. burnetii*. MCs were stimulated with *C. burnetii* (50 bacteria per cell) or left untreated for 8 h, and the total RNA was extracted prior to microarray analysis. (A) Up- and downregulated genes are indicated in red and green, respectively. (B) The (Continued on next page)

BMdMCs (Fig. 5K). These results indicated a direct cooperation between TLR4 and CD36 in the response of MCs to *C. burnetii*.

Role of CD36/TLR4 complex in cytoneme formation. Since the CD36/TLR4 cooperation is initiated by the interaction of *C. burnetii* with MCs, we wondered whether the CD36/TLR4 complex was involved in the formation of cytonemes. We therefore measured the cytoneme formation in response to *C. burnetii* in the presence of CD36 inhibitors. CD36 siRNA or CD36 blocking Abs inhibited cytoneme formation (Fig. 6A). Similarly, polymyxin B that inhibited CD36 expression (Fig. 5I) also prevented the formation of cytoneme. Finally, in TLR4-deficient BMdMCs stimulated by *C. burnetii*, an inhibition of 85% of cytoneme formation was observed (Fig. 6B). We then confirmed these results in primary MCs and showed that the treatment of pMCs with polymyxin B or CD36 blocking Abs inhibited cytoneme formation (Fig. 6C). Taken together, these results indicate that the release of cytoneme by MCs depends on cooperation between CD36 and TLR4 in response to the challenge of *C. burnetii*.

DISCUSSION

We have demonstrated here an antibacterial mechanism of MCs based on cytonemes that had never been reported before. It is established that bacteria are killed by innate immune cells via numerous intra- and extracellular mechanisms. The former are based on phagocytosis and phagosomal maturation, whereas the latter involve the formation of ETs and the release of bactericidal compounds (23). Microorganisms, including intracellular bacteria, have developed various strategies to subvert innate immune responses. Indeed, *C. burnetii* successfully infects macrophages by controlling phagocytosis and phagosome biogenesis (15, 24). We observed that MCs were able to kill *C. burnetii* without internalizing it, suggesting an extracellular microbicidal mechanism. This result is markedly distinct from *S. aureus*, which is killed by MCs via internalization and ET formation (6). While *C. burnetii* induces the formation of ETs as efficiently as *S. aureus* in neutrophils, *C. burnetii* is a poor inducer of ETs in MCs, which appeared insufficient to kill bacteria.

We also provided evidence that MCs use cytonemes for a microbicidal effect toward *C. burnetii*. Cytonemes were initially associated with cell-cell communication (25, 26). Although these cytoskeletal structures may participate in host defense, their specific antimicrobial role has not been described thus far. Cytonemes have been implicated in cell-to-cell spreading of virions, such as human immunodeficiency virus type 1 and human T cell leukemia virus type 1 (HTLV-1) (27, 28, 29). Recently, Hashimoto et al. reported that macrophage cytonemes enable the rapid transfer of HTLV-1 to surrounding cells (30). In contrast, neutrophil cytonemes are involved in the tethering of bacteria, such as *S. aureus*, *Salmonella enterica* serovar Typhimurium, and *Helicobacter pylori*. This capture of bacteria by neutrophil cytonemes allows internalization and subsequent intracellular destruction (31). The microbicidal activity of neutrophil cytonemes is probably based on the release of bactericidal molecules, such as lactoferrin, lipocalin, myeloperoxidase, defensins, and cathepsin G (32). We reported here that cytonemes entrapped *C. burnetii* and reduced its viability. The latter response is likely mediated by elastase and cathelicidin, which colocalized with bacteria within cytonemes. We also discovered that cytoneme-mediated killing of *C. burnetii* is associated with the absence of phagocytosis, whereas cytonemes and phagocytosis are associated, during the interaction of *S. aureus*, with MCs. The dissociation of cytoneme formation from phagocytosis was related to bacterial viability, since inactivated bacteria were internalized and did not induce significant cytoneme formation. The prevention

FIG 4 Legend (Continued)

relative distance between MCs stimulated with virulent *C. burnetii* (red), avirulent bacteria (green), or resting cells (blue) was assessed using principal-component analysis. (C) Venn diagrams showed the distribution of upregulated (left) and downregulated (right) genes in MCs stimulated with virulent *C. burnetii* (red) or avirulent variants (green). (D) Transcriptional analysis of modulated genes revealed several GO terms of biological process. (E) A modular analysis of the cell projection, immune response, and cytoskeletal organization of GO terms showed the genes involved and their modulation (up- and downregulation in red and blue, respectively).

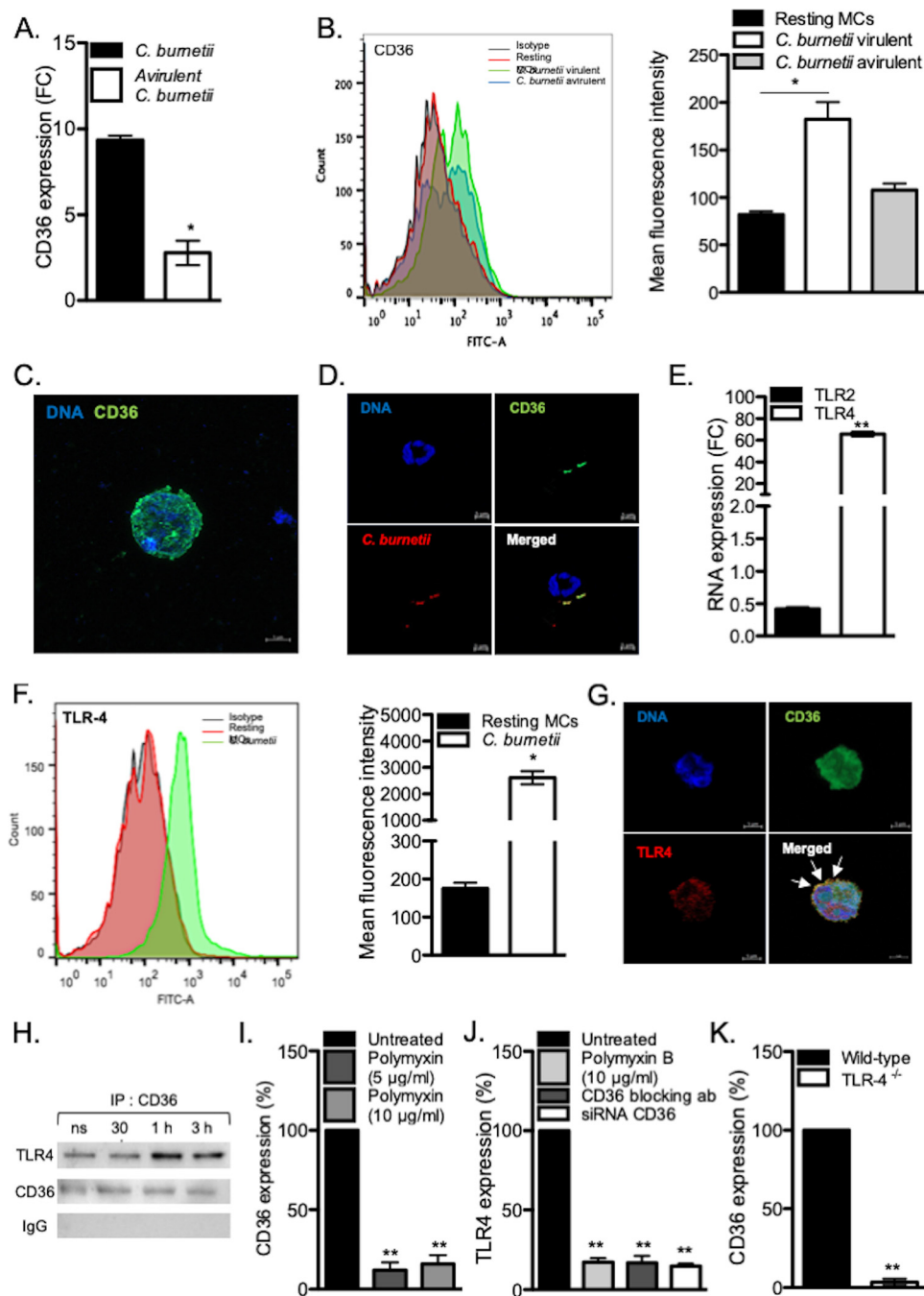


FIG 5 Involvement of CD36 and TLR4 in the response of MCs to *C. burnetii*. MCs were stimulated with *C. burnetii* or left untreated, and the modulation of the *CD36* and *TLR4* genes or encoded proteins was determined. (A) The expression of the gene encoding *CD36* was evaluated in MCs stimulated by *C. burnetii* for 8 h and normalized to the value for unstimulated cells. (B) The expression of *CD36* protein was determined by flow cytometry with FITC-conjugated anti-*CD36* on MCs stimulated with *C. burnetii* virulent and avirulent variants for 3 h. The results are expressed as mean fluorescence intensity. (C) Confocal microscopy revealed that the expression of *CD36* (green) was essentially expressed at the membrane. (D) The staining of *CD36* (green) and *C. burnetii* (red) showed that they colocalized (in yellow) at the MC membrane. (E) The expression of *TLR2* and *TLR4* transcripts was evaluated in MCs stimulated by *C. burnetii* for 8 h by qRT-PCR and normalized to the value for unstimulated cells. (F) The modulated expression of *TLR4* protein in response to *C. burnetii* was determined by flow cytometry and expressed as mean fluorescence intensity. (G) Confocal microscopy showed that *TLR4* (red) and *CD36* (green) colocalized (yellow) in *C. burnetii*-stimulated MCs (DNA appeared in blue). (H) MCs were stimulated with *C. burnetii* for different periods. Immunoprecipitations were immunoblotted with *TLR4*, *CD36*, or irrelevant Abs. (I and J) The expression of the *CD36* (I) and *TLR4* (J) genes was evaluated by qRT-PCR in MCs stimulated with *C. burnetii* for 8 h and treated with *CD36* blocking Abs or polymyxin B or after siRNACD36 transfection. The results are normalized to the values for untreated MCs. (K) The expression of *CD36* gene expression was assessed in *TLR4*^{-/-} BMDMCs and normalized to the value (Continued on next page)

Downloaded from <http://mbio.asm.org/> on November 12, 2020 by guest

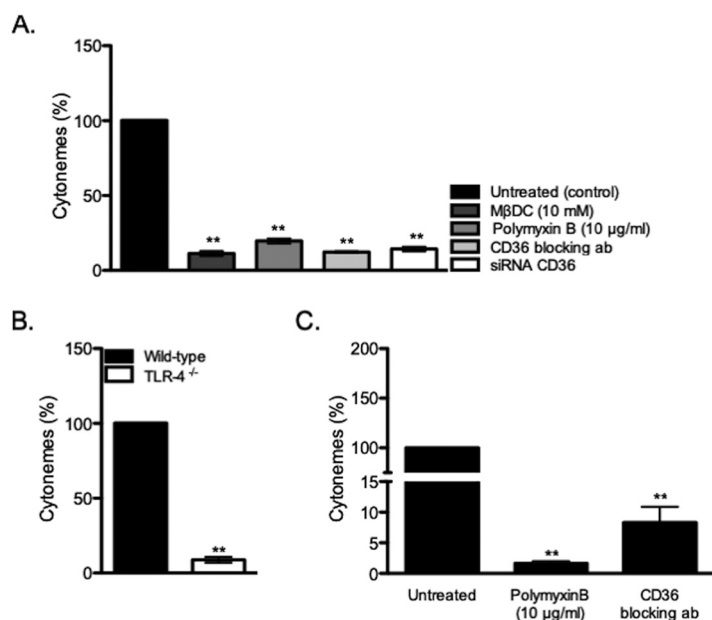


FIG 6 CD36/TLR4 cooperation. MCs were stimulated with *C. burnetii* for 3 h. (A) The percentage of cytonemes was calculated after treatment of stimulated MCs during 10 min with MβDC, polymyxin B, CD36 blocking Abs, or after siRNA CD36 transfection compared to untreated cells. (B) The percentage of cytonemes was calculated in TLR4-deficient BMDMCs compared to wild-type BMDMCs. (C) Placental MCs from healthy donors were collected after enzymatic digestion, Percoll cushion procedure, and magnetic selection. The release of cytonemes by pMCs stimulated by *C. burnetii* for 3 h were quantified after polymyxin B sulfate or CD36 blocking antibody treatments. Data are the means \pm SD for triplicate samples and are representative of four independent experiments. **, $P \leq 0.01$.

of phagocytosis in MCs is an active process reminiscent of what we reported in macrophages and monocytes infected with virulent *C. burnetii* (19, 33). Indeed, *C. burnetii* induced cytoskeletal reorganization of macrophages, such as F-actin protrusions, which was associated with phagocytosis prevention (10, 22). Manipulation of the cytoskeleton organization in macrophages restores phagocytosis, thus establishing a direct link between cytoskeleton modulation and phagocytosis interference (33, 34). We hypothesize that *C. burnetii*-induced cytonemes alert the immune system since it has been reported that externalized F-actin acts as a danger signal (35). Finally, in line with Manfredi et al. who proposed a choice between phagocytosis and generation of ETs for neutrophils during inflammation and infection (36), we think that MCs make a choice between MC formation and phagocytosis in the context of *C. burnetii* infection.

Our study also described that a functional cooperation between CD36 and TLRs is necessary for cytoneme formation. Indeed, we provide evidence that CD36 associates with TLR4, thus forming a molecular complex that is involved in the production of cytonemes and entrapping *C. burnetii*. This is consistent with previous reports in which CD36 mediated signal transduction for TLR4 (37, 38, 39). The role of CD36 in the immune response to microorganisms remains unclear. Some studies evoked a direct role of CD36 in inflammatory response or in pathogen recognition (40, 41). Indeed, Stuart et al. reported that CD36 may be a bacterial receptor for *S. aureus*, its cytoplasmic C-terminal extremity being involved in bacterial internalization (42). The transfection of CD36 into HeLa cells enhances the uptake of bacteria, including *Escherichia coli*, *Klebsiella pneumoniae*, *S. Typhimurium*, *S. aureus*, and *Enterococcus faecalis* (40). In addition, CD36 is involved in the internalization of LPS by endothelial or MCs (25, 43,

FIG 5 Legend (Continued)

for wild-type BMDMCs. Data are the means plus SD for triplicate samples from four independent experiments. *, $P \leq 0.05$; **, $P \leq 0.01$.

44). Future studies are required to address the precise mechanism underlying CD36/TLR4 cross talk during *C. burnetii* infection.

The formation of cytonemes in response to *C. burnetii* was not restricted to MC lines or murine MCs derived from bone marrow. It was also observed in primary MCs isolated from the human placenta. *C. burnetii* is known for its tropism for placenta tissue, and Q fever is a major risk for pregnancy and impaired fetal development (20). We previously described that *C. burnetii* interacts with dendritic cells from placenta and replicates in trophoblasts (11, 45). Here, we report that MCs from placenta present an extracellular mechanism to kill bacteria in the early phases of *C. burnetii* infection. The role of MCs in promoting host resistance in bacterial infection is documented (46–48). Thus, we can speculate that during *C. burnetii* infection, MCs play a role of protection at the placenta level by intercepting extracellular pathogens and limiting abortion. This finding may also explain why trophoblasts constitute a niche for *C. burnetii* (11). However, these hypotheses have to be clarified by careful examination of organism distribution in the naturally infected placenta in order to provide insights into the roles of individual cell types in abortion during Q fever.

In conclusion, our data described a new extracellular bactericidal mechanism based on the release of cytonemes by MCs. Cytonemes were involved in the capture of virulent *C. burnetii* and the destruction of entrapped bacteria mediated by antimicrobial peptides. We also showed that the formation of cytonemes requires the CD36/TLR4 complex. This report opens new perspectives in the antimicrobial activity of MCs and provides new insights into the role of cytonemes in the immune response.

MATERIALS AND METHODS

Cells. The human mast cell line HMC-1.2 was generously provided by M. Arock (Paris, France) and cultured in Iscove's modified Dulbecco's medium (IMDM) (Life Technologies) supplemented with 10% fetal bovine serum (FBS), 100 IU/ml penicillin, and 50 μ g/ml streptomycin (Life Technologies) at 37°C. In some experiments, placental MCs (pMCs) were isolated. Placenta from at-term healthy women were included after providing written informed consent and after approval was granted from the Comité d'Éthique d'Aix Marseille Université (number 08-012). Placenta tissue was digested with trypsin, and the cell suspension was deposited on a 25 to 60% Percoll cushion and centrifuged as previously described (49). Placental cells were collected, and pMCs were enriched by positive selection after Fc ϵ R1/CD117 staining (Miltenyi Biotec). In some experiments, bone marrow-derived MCs (BMDMCs) were differentiated as previously described (50). Briefly, wild-type mice were obtained from Charles River Laboratories, and TLR4-deficient mice were generously provided by L. Alexopoulou (Marseille, France). Bone marrow cells were flushed and incubated with IMDM containing 15% FBS, 10 ng/ml IL-3, and 10 ng/ml stem cell factor (Miltenyi Biotec). After 4 weeks of culture, the differentiation into BMDMCs was checked by flow cytometry using CD117 and Fc ϵ R1 as specific markers. About 98% of cultured cells were BMDMCs (data not shown). Human neutrophils and monocytes were isolated from blood samples from three healthy donors (Établissement Français du Sang, Marseille, France) using Percoll or Ficoll gradient, respectively, and incubated in RPMI 1640 (Life Technologies), as previously described (17).

Bacteria. Bacteria (Nine Mile and Guyana strains of *C. burnetii*) were prepared as previously reported (12). Avirulent variants of Nine Mile bacteria were obtained after repeated passages in L929 cells. Bacteria were stored at –80°C, their concentration was determined by Gimenez staining, and bacterial viability was assessed using the live/dead BacLight bacterial viability kit (Molecular Probes, Life Technologies) (51). Bacteria were inactivated at 95°C for 30 min. *S. aureus* (ATCC 25923) bacteria were grown on blood agar plates (bioMérieux) and quantified by flow cytometry (FACS BD Fortessa).

Cell stimulation. MCs and neutrophils (1×10^6 cells/well) were incubated in 24-well plates pretreated with fibronectin (1 mg/well; Life Technologies) for 3 h. Adherent cells were stimulated with 100 μ g/ml LPS, 25 nM phorbol-12-myristate-13-acetate (PMA) (MP Biomedicals), or bacteria (bacterium-to-cell ratio of 25 and 50 bacteria per cell for *S. aureus* and *C. burnetii*, respectively) at 37°C. The roles of CD36 and TLR4 were studied using MCs pretreated with 5 μ g/ml CD36-blocking antibodies (Abs) (mouse IgG2a; Thermo Fisher Scientific) or 10 μ g/ml of the TLR4 inhibitor polymyxin B sulfate (Sigma-Aldrich) for 10 min.

Bacterial detection. *C. burnetii* organisms were detected by quantitative PCR (qPCR) and immunofluorescence as previously described (12). The total DNA was extracted using the NucleoSpin kit (Macherey-Nagel). Quantitative PCR was performed using Sybr Green Technologies using a CFX (Bio-Rad) with 5 μ l of DNA and specific primers targeting *C. burnetii* *com1* gene: sense (5'-GCACTATTTTAGCCG GAACCTT-3') and antisense (5'-TTGAGGAGAAAACTGGATTGAGA-3'). *C. burnetii* organisms were also detected by immunofluorescence. In brief, MCs were fixed with 3% paraformaldehyde, permeabilized with 0.1% Triton X-100 for 5 min, and incubated with a 1/100 dilution of Q fever patient serum (11). After washing, MCs were incubated with Alexa Fluor 647-conjugated Abs. *S. aureus* was labeled with the fluorochrome DID (4-(4-(dihexadecylamino)styryl)-N-methylpyridinium iodide) (Thermo Fisher Scientific) for 20 min at 37°C.

Cytonemes and extracellular traps. The quantification of ET release was based on the evaluation of the area of labeled extracellular DNA filaments using an Axio Scan coupled with Hamamatsu sCOMS Flash 4 camera (Zeiss). The area of extracellular DNA of ETs was quantified on five different fields as previously described (52, 53). The results are expressed as a percentage relative to the PMA-stimulated cells as a positive control (cells stimulated with PMA) (54). Similarly, the evaluation of cytoneme formation over time was realized by assessment of area of extracellular F-actin filaments and expressed as a percentage relative to the PMA control, as depicted in Fig. S5 in the supplemental material. In some experiments, stimulated MCs were treated with 50 U/ml DNase (Sigma-Aldrich) for 30 min at the end of the experiment to disrupt ETs as previously described (17). The cytonemes were quantified using a similar method based on the release of extracellular F-actin labeled with phalloidin-488. To inhibit the formation of cytonemes, MCs were pretreated with 10 mM methyl- β -D-cyclodextrin (M β DC) (Sigma-Aldrich) for 10 min as previously described (18).

MC phenotyping and cytoneme staining. MCs were incubated with Abs directed against CD36 (mouse IgG1; Beckman Coulter), CD117 (mouse IgG1; Beckman Coulter), Fc ϵ R1 (mouse IgG1; Bühlmann Laboratories), TLR4 (mouse IgG1; BD Pharmingen), trypsin (mouse IgG1; Thermo Fisher Scientific), neutrophil elastase (rabbit IgG; Abcam), cathelicidin (rabbit IgG; Thermo Fisher Scientific), tubulin (mouse IgG1; Thermo Fisher Scientific), or appropriate isotype controls for 1 h. After the cells were washed, secondary Abs conjugated to Alexa Fluor 647 goat anti-rabbit or anti-mouse IgG1 (Life Technologies) were added to MCs for 30 min. Stained cells were then analyzed by confocal microscopy using an LSM 800 Airyscan confocal microscope (Zeiss) or by flow cytometry (10,000 events/acquisition) using a FACS BD Fortessa flow cytometer (BD Biosciences). The results of flow cytometry are expressed in mean fluorescence intensity (MFI), as calculated by the FlowJo software vX.0.7.

Microarray and data analysis. MCs (1×10^6 cells/well) were stimulated or not stimulated with *C. burnetii* for 8 h, and the total RNA was extracted using a RNeasy Mini kit followed by DNase treatment (Qiagen) to perform microarray experiment as described above (11). The 4X44K Human Whole Genome G4112F microarrays (Agilent Technologies), representing 45,000 probes, were used. Sample labeling and hybridization were performed using one-color microarray-based gene expression analysis. Four samples per experimental condition were included in the analysis. Slides were scanned with a pixel size of 5- μ m resolution with a G2505C DNA microarray scanner (Agilent Technologies), and data were analyzed with Feature Extraction Software 10.5.1. The selected probes were filtered for differentially expressed genes using an absolute fold change (FC) of ≥ 1.5 . The functional annotation was performed using DAVID Bioinformatics Resources (55, 56). The modulation of some genes was confirmed by quantitative reverse transcription-PCR (qRT-PCR) using the MMLV-RT kit (Life Technologies) and SYBR Green Fast Master Mix (Roche Diagnostics). Confirmation experiments were conducted using specific primers designed with Primer3 software (Table S1). The results were normalized using the housekeeping gene *actb* gene encoding β -actin and are expressed as the mean of $FC = 2^{-\Delta\Delta Ct}$ in which $\Delta\Delta Ct = (Ct_{Target} - Ct_{Actin})_{assay} - (Ct_{Target} - Ct_{Actin})_{control}$. The threshold cycle (Ct) was defined as the number of cycles required to detect the fluorescent signal. The expression of genes was considered modulated when the FC was ≥ 1.5 .

Small interference RNA transfection (siRNA). siRNAs directed against CD36 were purchased from Ambion (Life Technologies) and constructed with the following target sequences: sense (5'-CACUAUCAGUUGGAACAGAtt-3') and antisense (5'-UCUGUCCAACUGAUAGUaa-3'). HMC-1.2 cell line (1×10^6 cells/well) were grown to 80% confluence and transfected with 5 nM CD36 siRNA for 6 h using Lipofectamine 2000 (Life Technologies), according to the manufacturer's instructions (Life Technologies).

Immunoprecipitation. HMC-1.2 cells (1×10^7 cells) were treated with *C. burnetii* (50 bacteria per cell) for the indicated periods, washed in ice-cold phosphate-buffered saline and lysed in 20 mM Tris-HCl (pH 7.4), 200 mM NaCl, 1 mM EDTA, 1% Triton X-100 with protease inhibitors as previously described (41). Protein lysate was incubated with 4 μ g of anti-human CD36 (Thermo Fisher Scientific) or control IgG (mouse IgG2a; Beckman Coulter) overnight at 4°C and then incubated with protein G-Sepharose beads (Sigma-Aldrich) for 3 h at 4°C. Immunoblotting was performed on 10% polyacrylamide gels using anti-CD36 (rabbit IgG; Thermo Fisher Scientific) and anti-TLR4 (rabbit IgG; Thermo Fisher Scientific) Abs, and the signal were recorded using the ECL Plus reagent (Thermo Fisher Scientific).

Statistical analysis. Data were analyzed with GraphPad Prism 5.0c and Student's *t* test. A *P* value of < 0.05 was considered statistically significant.

Accession number(s). The data have been deposited in NCBI's Gene Expression Omnibus (57) and are accessible through GEO series accession number [GSE111971](https://www.ncbi.nlm.nih.gov/geo/query/acc.cgi?acc=GSE111971).

SUPPLEMENTAL MATERIAL

Supplemental material for this article may be found at <https://doi.org/10.1128/mBio.02669-18>.

FIG S1, PDF file, 1.9 MB.

FIG S2, PDF file, 0.03 MB.

FIG S3, PDF file, 1.2 MB.

FIG S4, PDF file, 0.03 MB.

FIG S5, PDF file, 0.03 MB.

TABLE S1, PDF file, 0.01 MB.

TABLE S2, PDF file, 0.03 MB.

ACKNOWLEDGMENTS

We thank Pascal Weber for his assistance with confocal microscopy, Jacques Bou Khalil and Jean-Pierre Baudoin for their contributions to electron microscopy experiments, and Malgorzata Kowalczywska for her contributions to immunoblot assays. We are grateful to Lena Alexopoulou (CIML, Marseille, France) and Michel Arock (Paris, France) for providing us with the TLR4 knockout mice and HMC-1.2 cell line, respectively. We thank Christian Capo for his help and advice in writing the manuscript.

Soraya Mezouar was supported by a personal grant from the “Fondation pour la Recherche Médicale” (FRM) postdoctoral fellowship (SPF20151234951).

This work was supported by technical support, including the French Government under the “Investissements d’avenir” (Investments for the Future) program managed by the “Agence Nationale de la Recherche” (reference Méditerranée Infection 10-IAHU-03) and the Région Provence-Alpes-Côte d’Azur and the European funding FEDER PRIMI.

S.M. and J.-L.M. conceived and designed the experiments. S.M., L.G., B.D., and A.B.A. performed experiments, and S.M., L.G., and A.B.A. analyzed the data. S.M., J.V., B.D., and J.-L.M. wrote the paper.

We declare that we have no competing interests.

REFERENCES

- Sayed BA, Christy A, Quirion MR, Brown MA. 2008. The master switch: the role of mast cells in autoimmunity and tolerance. *Annu Rev Immunol* 26:705–739. <https://doi.org/10.1146/annurev.immunol.26.021607.090320>.
- Abraham SN, St John AL. 2010. Mast cell-orchestrated immunity to pathogens. *Nat Rev Immunol* 10:440–452. <https://doi.org/10.1038/nri2782>.
- Sandig H, Bulfone-Paus S. 2012. TLR signaling in mast cells: common and unique features. *Front Immunol* 3:185. <https://doi.org/10.3389/fimmu.2012.00185>.
- Kawasaki T, Kawai T. 2014. Toll-like receptor signaling pathways. *Front Immunol* 5:461. <https://doi.org/10.3389/fimmu.2014.00461>.
- Frank BT, Rossall JC, Caughey GH, Fang KC. 2001. Mast cell tissue inhibitor of metalloproteinase-1 is cleaved and inactivated extracellularly by α -chymase. *J Immunol* 166:2783–2792. <https://doi.org/10.4049/jimmunol.166.4.2783>.
- Malaviya R, Twisten NJ, Ross EA, Abraham SN, Pfeifer JD. 1996. Mast cells process bacterial Ags through a phagocytic route for class I MHC presentation to T cells. *J Immunol* 156:1490–1496.
- von Köckritz-Blickwede M, Goldmann O, Thulin P, Heinemann K, Norrby-Teglund A, Rohde M, Medina E. 2008. Phagocytosis-independent antimicrobial activity of mast cells by means of extracellular trap formation. *Blood* 111:3070–3080. <https://doi.org/10.1182/blood-2007-07-104018>.
- Eldin C, Mélenotte C, Mediannikov O, Ghigo E, Million M, Edouard S, Mege J-L, Maurin M, Raoult D. 2017. From Q fever to *Coxiella burnetii* infection: a paradigm change. *Clin Microbiol Rev* 30:115–190. <https://doi.org/10.1128/CMR.00045-16>.
- Shannon JG, Howe D, Heinzen RA. 2005. Virulent *Coxiella burnetii* does not activate human dendritic cells: role of lipopolysaccharide as a shielding molecule. *Proc Natl Acad Sci U S A* 102:8722–8727. <https://doi.org/10.1073/pnas.0501863102>.
- Benoit M, Barbarat B, Bernard A, Olive D, Mege J-L. 2008. *Coxiella burnetii*, the agent of Q fever, stimulates an atypical M2 activation program in human macrophages. *Eur J Immunol* 38:1065–1070. <https://doi.org/10.1002/eji.200738067>.
- Ben Amara A, Ghigo E, Le Priol Y, Lépolard C, Salcedo SP, Lemichez E, Bretelle F, Capo C, Mege J-L. 2010. *Coxiella burnetii*, the agent of Q fever, replicates within trophoblasts and induces a unique transcriptional response. *PLoS One* 5:e15315. <https://doi.org/10.1371/journal.pone.0015315>.
- Bechah Y, Verneau J, Ben Amara A, Barry AO, Lépolard C, Achard V, Panicot-Dubois L, Textoris J, Capo C, Ghigo E, Mege J-L. 2014. Persistence of *Coxiella burnetii*, the agent of Q fever, in murine adipose tissue. *PLoS One* 9:e97503. <https://doi.org/10.1371/journal.pone.0097503>.
- Amara AB, Bechah Y, Mege J-L. 2012. Immune response and *Coxiella burnetii* invasion. *Adv Exp Med Biol* 984:287–298. https://doi.org/10.1007/978-94-007-4315-1_15.
- Capo C, Lindberg FP, Meconi S, Zaffran Y, Tardei G, Brown EJ, Raoult D, Mege J-L. 1999. Subversion of monocyte functions by *Coxiella burnetii*: impairment of the cross-talk between α v β 3 integrin and CR3. *J Immunol* 163:6078–6085.
- Abnave P, Muraccione X, Ghigo E. 2017. *Coxiella burnetii* lipopolysaccharide: what do we know? *Int J Mol Sci* 18:E2509. <https://doi.org/10.3390/ijms18122509>.
- Dellacasagrande J, Ghigo E, Hammami SM, Toman R, Raoult D, Capo C, Mege JL. 2000. α (v) β (3) integrin and bacterial lipopolysaccharide are involved in *Coxiella burnetii*-stimulated production of tumor necrosis factor by human monocytes. *Infect Immun* 68:5673–5678. <https://doi.org/10.1128/IAI.68.10.5673-5678.2000>.
- Thomas GM, Brill A, Mezouar S, Crescence L, Gallant M, Dubois C, Wagner DD. 2015. Tissue factor expressed by circulating cancer cell-derived microparticles drastically increases the incidence of deep vein thrombosis in mice. *J Thromb Haemost* 13:1310–1319. <https://doi.org/10.1111/jth.13002>.
- Fifadara NH, Beer F, Ono S, Ono SJ. 2010. Interaction between activated chemokine receptor 1 and Fc ϵ RI at membrane rafts promotes communication and F-actin-rich cytoneme extensions between mast cells. *Int Immunol* 22:113–128. <https://doi.org/10.1093/intimm/dxp118>.
- Meconi S, Jacomo V, Boquet P, Raoult D, Mege JL, Capo C. 1998. *Coxiella burnetii* induces reorganization of the actin cytoskeleton in human monocytes. *Infect Immun* 66:5527–5533.
- Nielsen SY, Mølbak K, Henriksen TB, Krogfelt KA, Larsen CS, Villumsen S. 2014. Adverse pregnancy outcomes and *Coxiella burnetii* antibodies in pregnant women, Denmark. *Emerg Infect Dis* 20:925–931. <https://doi.org/10.3201/eid2006.130584>.
- Canton J, Neculai D, Grinstein S. 2013. Scavenger receptors in homeostasis and immunity. *Nat Rev Immunol* 13:621–634. <https://doi.org/10.1038/nri3515>.
- Honstetter A, Ghigo E, Moynault A, Capo C, Toman R, Akira S, Takeuchi O, Lepidi H, Raoult D, Mege J-L. 2004. Lipopolysaccharide from *Coxiella burnetii* is involved in bacterial phagocytosis, filamentous actin reorganization, and inflammatory responses through Toll-like receptor 4. *J Immunol* 172:3695–3703. <https://doi.org/10.4049/jimmunol.172.6.3695>.
- Agier J, Brzezińska-Błaszczak E. 2016. Cathelicidins and defensins regulate mast cell antimicrobial activity. *Postepy Hig Med Dosw (Online)* 70:618–636. <https://doi.org/10.5604/10.5604/17322693.1205357>.
- Abnave P, Mottola G, Gimenez G, Boucherit N, Trouplin V, Torre C, Conti F, Ben Amara A, Lepolard C, Djian B, Hamaoui D, Mettouchi A, Kumar A, Pagnotta S, Bonatti S, Lepidi H, Salvetti A, Abi-Rached L, Lemichez E, Mege J-L, Ghigo E. 2014. Screening in planarians identifies MORN2 as a key component in LC3-associated phagocytosis and resistance to bacterial infection. *Cell Host Microbe* 16:338–350. <https://doi.org/10.1016/j.chom.2014.08.002>.
- Marshall JS. 2004. Mast-cell responses to pathogens. *Nat Rev Immunol* 4:787–799. <https://doi.org/10.1038/nri1460>.

26. Sherer NM, Mothes W. 2008. Cytonemes and tunneling nanotubules in cell–cell communication and viral pathogenesis. *Trends Cell Biol* 18: 414–420. <https://doi.org/10.1016/j.tcb.2008.07.003>.
27. Sherer NM, Lehmann MJ, Jimenez-Soto LF, Horensavitz C, Pypaert M, Mothes W. 2007. Retroviruses can establish filopodial bridges for efficient cell-to-cell transmission. *Nat Cell Biol* 9:310–315. <https://doi.org/10.1038/ncb1544>.
28. Alfsen A, Yu H, Magéus-Chatinet A, Schmitt A, Bomsel M. 2005. HIV-1-infected blood mononuclear cells form an integrin- and agrin-dependent viral synapse to induce efficient HIV-1 transcytosis across epithelial cell monolayer. *Mol Biol Cell* 16:4267–4279. <https://doi.org/10.1091/mbc.e05-03-0192>.
29. Sowinski S, Jolly C, Berninghausen O, Purbhoo MA, Chauveau A, Köhler K, Oddos S, Eissmann P, Brodsky FM, Hopkins C, Onfelt B, Sattentau Q, Davis DM. 2008. Membrane nanotubes physically connect T cells over long distances presenting a novel route for HIV-1 transmission. *Nat Cell Biol* 10:211–219. <https://doi.org/10.1038/ncb1682>.
30. Hashimoto M, Bhuyan F, Hiyoshi M, Noyori O, Nasser H, Miyazaki M, Saito T, Kondoh Y, Osada H, Kimura S, Hase K, Ohno H, Suzu S. 2016. Potential role of the formation of tunneling nanotubes in HIV-1 spread in macrophages. *J Immunol* 196:1832–1841. <https://doi.org/10.4049/jimmunol.1500845>.
31. Corriden R, Self T, Akong-Moore K, Nizet V, Kellam B, Briddon SJ, Hill SJ. 2013. Adenosine-A3 receptors in neutrophil microdomains promote the formation of bacteria-tethering cytonemes. *EMBO Rep* 14:726–732. <https://doi.org/10.1038/embor.2013.89>.
32. Galkina SI, Fedorova NV, Serebryakova MV, Romanova JM, Golyshev SA, Stadnichuk VI, Baratova LA, Sud'ina GF, Klein T. 2012. Proteome analysis identified human neutrophil membrane tubulovesicular extensions (cytonemes, membrane tethers) as bactericide trafficking. *Biochim Biophys Acta* 1820:1705–1714. <https://doi.org/10.1016/j.bbagen.2012.06.016>.
33. Meconi S, Capo C, Remacle-Bonnet M, Pommier G, Raoult D, Mege J-L. 2001. Activation of protein tyrosine kinases by *Coxiella burnetii*: role in actin cytoskeleton reorganization and bacterial phagocytosis. *Infect Immun* 69:2520–2526. <https://doi.org/10.1128/IAI.69.4.2520-2526.2001>.
34. Conti F, Boucherit N, Baldassarre V, Trouplin V, Toman R, Mottola G, Mege J-L, Ghigo E. 2015. *Coxiella burnetii* lipopolysaccharide blocks p38 α -MAPK activation through the disruption of TLR-2 and TLR-4 association. *Front Cell Infect Microbiol* 4:182. <https://doi.org/10.3389/fcimb.2014.00182>.
35. Mostowy S, Shenoy AR. 2015. The cytoskeleton in cell-autonomous immunity: structural determinants of host defence. *Nat Rev Immunol* 15:559–573. <https://doi.org/10.1038/nri3877>.
36. Manfredi AA, Ramirez GA, Rovere-Querini P, Maugeri N. 2018. The neutrophil's choice: phagocytose vs make neutrophil extracellular traps. *Front Immunol* 9:288. <https://doi.org/10.3389/fimmu.2018.00288>.
37. Hoebe K, Georgel P, Rutschmann S, Du X, Mudd S, Crozat K, Sovath S, Shamel L, Hartung T, Zähringer U, Beutler B. 2005. CD36 is a sensor of diacylglycerides. *Nature* 433:523–527. <https://doi.org/10.1038/nature03253>.
38. Triantafilou M, Gamper FGJ, Haston RM, Mouratis MA, Morath S, Hartung T, Triantafilou K. 2006. Membrane sorting of Toll-like receptor (TLR)-2/6 and TLR2/1 heterodimers at the cell surface determines heterotypic associations with CD36 and intracellular targeting. *J Biol Chem* 281: 31002–31011. <https://doi.org/10.1074/jbc.M602794200>.
39. Wright SD, Ramos RA, Tobias PS, Ulevitch RJ, Mathison JC. 1990. CD14, a receptor for complexes of lipopolysaccharide (LPS) and LPS binding protein. *Science* 249:1431–1433. <https://doi.org/10.1126/science.1698311>.
40. Baranova IN, Kurlander R, Bocharov AV, Vishnyakova TG, Chen Z, Remaley AT, Csako G, Patterson AP, Eggerman TL. 2008. Role of human CD36 in bacterial recognition, phagocytosis, and pathogen-induced JNK-mediated signaling. *J Immunol* 181:7147–7156. <https://doi.org/10.4049/jimmunol.181.10.7147>.
41. Cao D, Luo J, Chen D, Xu H, Shi H, Jing X, Zang W. 2016. CD36 regulates lipopolysaccharide-induced signaling pathways and mediates the internalization of *Escherichia coli* in cooperation with TLR4 in goat mammary gland epithelial cells. *Sci Rep* 6:23132. <https://doi.org/10.1038/srep23132>.
42. Stuart LM, Deng J, Silver JM, Takahashi K, Tseng AA, Hennessy EJ, Ezekowitz RAB, Moore KJ. 2005. Response to *Staphylococcus aureus* requires CD36-mediated phagocytosis triggered by the COOH-terminal cytoplasmic domain. *J Cell Biol* 170:477–485. <https://doi.org/10.1083/jcb.200501113>.
43. Hampton RY, Golenbock DT, Penman M, Krieger M, Raetz CR. 1991. Recognition and plasma clearance of endotoxin by scavenger receptors. *Nature* 352:342–344. <https://doi.org/10.1038/352342a0>.
44. Vishnyakova TG, Bocharov AV, Baranova IN, Chen Z, Remaley AT, Csako G, Eggerman TL, Patterson AP. 2003. Binding and internalization of lipopolysaccharide by Cla-1, a human orthologue of rodent scavenger receptor B1. *J Biol Chem* 278:22771–22780. <https://doi.org/10.1074/jbc.M211032200>.
45. Gorvel L, Ben Amara A, Ka MB, Textoris J, Gorvel JP, Mege JL. 2014. Myeloid decidual dendritic cells and immunoregulation of pregnancy: defective responsiveness to *Coxiella burnetii* and *Brucella abortus*. *Front Cell Infect Microbiol* 4:179. <https://doi.org/10.3389/fcimb.2014.00179>.
46. Piliponsky AM, Chen C-C, Grimbaldeston MA, Burns-Guydish SM, Hardy J, Kalesnikoff J, Contag CH, Tsai M, Galli SJ. 2010. Mast cell-derived TNF can exacerbate mortality during severe bacterial infections in C57BL/6-KitW^{sh}/W^{sh} mice. *Am J Pathol* 176:926–938. <https://doi.org/10.2353/ajpath.2010.090342>.
47. Thakurdas SM, Melicoff E, Sansores-Garcia L, Moreira DC, Petrova Y, Stevens RL, Adachi R. 2007. The mast cell-restricted tryptase mMCP-6 has a critical immunoprotective role in bacterial infections. *J Biol Chem* 282:20809–20815. <https://doi.org/10.1074/jbc.M611842200>.
48. Kalesnikoff J, Galli SJ. 2008. New developments in mast cell biology. *Nat Immunol* 9:1215–1223. <https://doi.org/10.1038/nif.216>.
49. Mezouar S, Ben Amara A, Vitte J, Mege J-L. 2018. Isolation of human placental mast cells. *Curr Protoc Cell Biol* 80:e52. <https://doi.org/10.1002/cpcb.52>.
50. Abel J, Goldmann O, Ziegler C, Höltje C, Smeltzer MS, Cheung AL, Bruhn D, Rohde M, Medina E. 2011. *Staphylococcus aureus* evades the extracellular antimicrobial activity of mast cells by promoting its own uptake. *J Innate Immun* 3:495–507. <https://doi.org/10.1159/000327714>.
51. Ka MB, Mezouar S, Ben Amara A, Raoult D, Ghigo E, Olive D, Mege JL. 2016. *Coxiella burnetii* induces inflammatory interferon-like signature in plasmacytoid dendritic cells: a new feature of immune response in Q fever. *Front Cell Infect Microbiol* 6:70. <https://doi.org/10.3389/fcimb.2016.00070>.
52. Kraaij T, Cowling RM, van Wilgen BW, Rikhotso DR, Difford M. 2017. Vegetation responses to season of fire in an aseasonal, fire-prone fynbos shrubland. *PeerJ* 5:e3591. <https://doi.org/10.7717/peerj.3591>.
53. Rebernick R, Fahmy L, Glover C, Bawadekar M, Shim D, Holmes CL, Rademacher N, Potluri H, Bartels CM, Shelef MA. 2018. DNA Area and NETosis Analysis (DNA): a high-throughput method to quantify neutrophil extracellular traps in fluorescent microscope images. *Biol Proced Online* 20:7. <https://doi.org/10.1186/s12575-018-0072-y>.
54. White PC, Chicca IJ, Ling MR, Wright HJ, Cooper PR, Milward MR, Chapple ILC. 2017. Characterization, quantification, and visualization of neutrophil extracellular traps. *Methods Mol Biol* 1537:481–497. https://doi.org/10.1007/978-1-4939-6685-1_29.
55. Larkin JE, Frank BC, Gavras H, Sultana R, Quackenbush J. 2005. Independence and reproducibility across microarray platforms. *Nat Methods* 2:337–344. <https://doi.org/10.1038/nmeth757>.
56. Bammmler T, Beyer RP, Bhattacharya S, Boorman GA, Boyles A, Bradford BU, Bumgarner RE, Bushel PR, Chaturvedi K, Choi D, Cunningham ML, Deng S, Dressman HK, Fannin RD, Farin FM, Freedman JH, Fry RC, Harper A, Humble MC, Hurban P, Kavanagh TJ, Kaufmann WK, Kerr KF, Jing L, Lapidus JA, Lasarev MR, Li J, Li Y-J, Lobenhofer EK, Lu X, Malek RL, Milton S, Nagalla SR, O'Malley JP, Palmer VS, Pattee P, Puares RS, Perou CM, Phillips K, Qin L-X, Qiu Y, Quigley SD, Rodland M, Rusyn I, Samson LD, Schwartz DA, Shi Y, Shin J-L, Sieber SO, Slifer S, Speer MC, et al. 2005. Standardizing global gene expression analysis between laboratories and across platforms. *Nat Methods* 2:351–356.
57. Barrett T, Edgar R. 2006. Gene expression omnibus: microarray data storage, submission, retrieval, and analysis. *Methods Enzymol* 411: 352–369. [https://doi.org/10.1016/S0076-6879\(06\)11019-8](https://doi.org/10.1016/S0076-6879(06)11019-8).